Angle/Doppler Estimation in Heavy-Tailed Clutter Backgrounds

PANAGIOTIS TSAKALIDES, Member, IEEE
RAFFAELE RASPANTI
CHRYSOSTOMOS L. NIKIAS, Fellow, IEEE
University of Southern California

This work describes new methods on the modeling of the amplitude statistics of airborne radar clutter by means of alpha-stable distributions. We develop joint target angle and Doppler, maximum likelihood-based estimation techniques from radar measurements retrieved in the presence of impulsive uncorrelated noise modeled as an alpha-stable random process. We derive the Cramér–Rao bounds (CRBs) for the additive Cauchy interference scenario to assess the best case estimation accuracy which can be achieved. In addition, we introduce a new joint spatial- and Doppler-frequency high-resolution estimation technique based on the fractional lower order statistics of the measurements of a radar array. Simulation results demonstrate that the proposed methods can be of interest in the study of space-time adaptive processing (STAP) for airborne pulse Doppler radar arrays operating in impulsive interference environments.

Manuscript received May 23, 1996; revised May 12, 1998.

IEEE Log No. T-AES/35/2/04297.

This work was supported by Rome Laboratory under Contract F30602-95-1-0001 and by the Office of Naval Research under Contract N00014-92-J-1034.

Authors' current addresses: P. Tsakalides, VLSI Design Laboratory, Electrical and Computer Engineering Department, University of Patras, Rio 265 00, Greece; R. Raspanti, Andersen Consulting, Rome, Italy; C. L. Nikias, Signal and Image Processing Institute, Dept. of Electrical Engineering Systems, University of Southern California, EEB Room 400, 3740 McClintock Ave., Los Angeles, CA 90089-2564.

0018-9251/99/$10.00

I. INTRODUCTION

Future advanced airborne radar systems must be able to detect, identify, and estimate the parameters of a target in severe interference backgrounds. As a result, the problem of clutter and jamming suppression has been the focus of considerable research in the radar engineering community. In the early 1970s, Reed, Mallett, and Brennan developed a theory for adaptive weight computation of a processor which maximizes the probability of detection for a fixed false-alarm rate [1, 2]. Later, Kelly addressed the problem of determining the detector threshold to achieve a given probability of false alarm which is independent of the covariance matrix, i.e., the level and structure of the noise [3].

Most of the theoretical work in detection and estimation for radar applications has focused on the case where the clutter is assumed to follow the Gaussian model. The Gaussian assumption is frequently motivated by the physics of the problem and it often leads to mathematically tractable solutions. However, it has been recognized that effective clutter suppression can be achieved only on the basis of appropriate statistical modeling. Indeed, the radar community has studied the non-Gaussian characteristics of clutter by considering alternative statistical models such as the K [4], the Weibull [5, 6], and the log-normal [7] distributions. As a result, detection schemes have been developed by taking into consideration the non-Gaussian modeling of the data. Kassam developed robust detectors for mixture noise classes [8], while Goldman studied the detection problem in spherically invariant noise which he considered as a natural generalization of Gaussian noise [9].

Consequently, Sangston and Gerlach derived both optimal and suboptimal receivers for clutter modeled by a mixture of Rayleigh distributions [10]. Rangaswamy, et al. studied the radar detection and identification problems by using a general class of spherically invariant random processes [11]. Related work was also performed by Izzo and Tanda [12, 13]. Recently, experimental results have been reported where clutter returns have a heavy-tailed nature [14]. In addition, a statistical model of impulsive interference has been proposed, which is based on the theory of symmetric alpha-stable (SαS) random processes [15]. The model is of a statistical-physical nature and has been shown to arise under very general assumptions and to describe a broad class of impulsive interference.

Space Time Adaptive Processing (STAP) has been introduced as a generalization of displaced-phase-center antenna (DPCA) processing and has been recognized as the technology which will enable long-range detection of increasingly smaller targets in the presence of severe clutter and jamming [16]. STAP refers to adaptive antenna processors that simultaneously combine the signals received on multiple elements of an antenna array and from multiple pulse repetition periods of a radar coherent processing interval [17]. In other words, the STAP processor can be viewed as a two-dimensional (2-D) filter which performs both beamforming (spatial filtering) and Doppler (temporal) filtering to suppress interference and achieve target detection and parameter estimation. As a result, several researchers have concentrated their efforts on the theoretical advancement and understanding of the various aspects of the STAP discipline such as partially adaptive STAP [17], pre-Doppler processing for adaptive clutter nulling [18], detection in undernulled clutter [19], and non-Gaussian STAP [20].

As pointed out by Ward in [21], much of the work reported for radar systems has concentrated on target *detection* in Gaussian or non-Gaussian backgrounds. We address the target *parameter estimation* problem through the use of STAP radar array sensor data retrieved in the presence of impulsive interference of an uncorrelated nature. In particular, we derive Cramér–Rao bounds (CRBs) on angle and Doppler estimator accuracy for the case of additive Cauchy noise. In addition, we present a new subspace-based method for joint spatial- and Doppler-frequency high-resolution estimation in the presence of uncorrelated heavy-tailed noise. The results obtained here can be viewed as generalizations of the work done in [22, 23] to the 2-D frequency estimation problem in impulsive interference backgrounds.

The paper is organized in six sections. In Section II, we present some necessary preliminaries on α-stable processes and results on the modeling of real clutter data by means of SαS distributions. In Section III, we formulate the STAP problem for airborne radar. In Section IV, we form the maximum likelihood (ML) function, we present the Cramér–Rao analysis, and we derive bounds on the variances of the spatial and temporal frequency estimates. In Section V, we define the covariation matrix of the space-time radar sensor output snapshot and we show that eigendecomposition-based methods, such as the multiple signal classification (MUSIC) algorithm, can be applied to the sample covariation matrix to extract the angle/Doppler information from the measurements. Finally, in Section VI, the improved performance of the proposed target parameter estimation methods in the presence of a wide range of impulsive noise environments is demonstrated via Monte Carlo experiments.

II. MATHEMATICAL PRELIMINARIES: SYMMETRIC ALPHA-STABLE DISTRIBUTIONS

In this section, we introduce the statistical model that is used to describe the additive noise. The model is based on the class of *isotropic* SαS distributions, and is well suited for describing impulsive noise processes [15].

Stable processes satisfy the stability property which states that linear combinations of jointly stable variables are indeed stable. They arise as limiting processes of sums of independent, identically distributed random variables (RVs) via the generalized Central Limit Theorem. They are described by their characteristic exponent α, taking values $0 < \alpha \leq 2$. Gaussian processes are stable processes with $\alpha = 2$. Stable distributions have heavier tails than the normal distribution, possess finite pth-order moments only for $p < \alpha$, and are appropriate for modeling noise with outliers.

A complex RV $X = X_1 + jX_2$ is isotropic SαS if X_1 and X_2 are jointly SαS and have a symmetric distribution, i.e., a distribution which is circularly invariant with respect to their location parameter. The characteristic function of X is given by

$$\varphi(\omega) = \mathcal{E}\{\exp(j\Re[\omega X^*])\} = \exp(-\gamma|\omega|^\alpha) \tag{1}$$

where $\omega = \omega_1 + j\omega_2$, $\mathcal{E}\{\cdot\}$ is the statistical expectation operator, $\Re[\cdot]$ is the real part operator, and $*$ denotes complex conjugate. The *characteristic exponent* α is restricted to the values $0 < \alpha \leq 2$ and it determines the shape of the distribution. The smaller the characteristic exponent α, the heavier the tails of the density. The *dispersion* γ ($\gamma > 0$) plays a role analogous to the role that the variance plays for second-order processes. Namely, it determines the spread of the probability density function around the origin.

Several complex RVs are jointly SαS if their real and imaginary parts are jointly SαS. When $X = X_1 + jX_2$ and $Y = Y_1 + jY_2$ are jointly SαS with $1 < \alpha \leq 2$, the *covariation* of X and Y is defined by

$$[X,Y]_\alpha = \int_{S_4} (x_1 + jx_2)(y_1 + jy_2)^{\langle\alpha-1\rangle} d\Gamma_{X_1,X_2,Y_1,Y_2}(x_1,x_2,y_1,y_2) \tag{2}$$

where Γ_{X_1,X_2,X_3,X_4} is the *spectral measure*, symmetric on the unit hyper-sphere S_4. We use throughout the convention:

$$Y^{\langle\beta\rangle} = |Y|^{\beta-1}Y^*. \tag{3}$$

It can be shown that for every $1 \leq p < \alpha$, the covariation can be expressed as a function of moments [24]

$$[X,Y]_\alpha = \frac{E\{XY^{\langle p-1\rangle}\}}{E\{|Y|^p\}}\gamma_Y \tag{4}$$

where γ_Y is the dispersion of the RV Y given by

$$\gamma_Y^{p/\alpha} = \frac{E\{|Y|^p\}}{C(p,\alpha)} \quad \text{for} \quad 0 < p < \alpha \tag{5}$$

with

$$C(p,\alpha) = \frac{2^{p+1}\Gamma\left(\frac{p+2}{2}\right)\Gamma\left(-\frac{p}{\alpha}\right)}{\alpha\Gamma\left(\frac{1}{2}\right)\Gamma\left(-\frac{p}{2}\right)} \tag{6}$$

where $\Gamma(\cdot)$ is the gamma function defined by

$$\Gamma(x) = \int_0^\infty t^{x-1} e^{-t} dt. \qquad (7)$$

Obviously, from (4) it holds that

$$[X,X]_\alpha = \gamma_X. \qquad (8)$$

Also, the *covariation coefficient* of X and Y is defined by

$$\lambda_{X,Y} = \frac{[X,Y]_\alpha}{[Y,Y]_\alpha} \qquad (9)$$

and by using (4), it can be expressed as

$$\lambda_{X,Y} = \frac{\mathcal{E}\{XY^{\langle p-1\rangle}\}}{\mathcal{E}\{|Y|^p\}}, \qquad \text{for} \quad 1 \le p < \alpha. \qquad (10)$$

The covariation of complex jointly SαS RVs is not generally symmetric and has the following properties [25].

P1: If X_1, X_2 and Y are jointly SαS, then for any complex constants a and b,

$$[aX_1 + bX_2, Y]_\alpha = a[X_1,Y]_\alpha + b[X_2,Y]_\alpha.$$

P2: If Y_1 and Y_2 are independent and X_1, X_2, and Y are jointly SαS, then for any complex constants a, b, and c,

$$[aX_1, bY_1 + cY_2]_\alpha = ab^{\langle \alpha-1\rangle}[X_1,Y_1]_\alpha + ac^{\langle \alpha-1\rangle}[X_1,Y_2]_\alpha.$$

P3: If X and Y are independent SαS, then $[X,Y]_\alpha = 0$.

Typically, the statistics of real radar clutter data are unknown. The possibility that heavy-tailed clutter behavior may adequately be described by the stable laws gives rise to the need for fast, simple, and efficient estimators of the alpha-stable parameters (especially, the characteristic exponent α) from real data. Several such estimators compromising optimality for the sake of computational efficiency, have been proposed in the past. Among them, ML methods developed by DuMouchel [26] and by Brorsen and Yang [27] are asymptotically efficient but difficult to compute. Paulson, et al. estimate the stable parameters by fitting the Fourier transform of the data to the characteristic function [28], a computer-intensive procedure. Hence, a number of suboptimal but simple methods have been devised. Zolotarev estimates the stable parameters by the method of moments, but requires that the location parameter is known in advance [29]. Brockwell and Brown estimate α with high efficiency in the special case of $\alpha < 1$. MuCullogh [30] generalized the Famma and Roll approach [31] to provide consistent estimators of α in the range [0.6,2].

Figs. 1 and 2 show results on the modeling of the amplitude statistics of real sea clutter by means of SαS distributions. The data were provided by the Naval Surface Warfare Center, Carderock Division, Bethesda, MD. The sea clutter data were taken in a sea state 3 with an X-band radar at an 8° look-down angle with a spatial resolution of 1.52 m (5 ft) sampled at 40 Hz, representing a nominal sea condition. A comparison is made between the SαS amplitude probability density (APD) and the Gaussian APD on how they approximate the empirical APD corresponding to the real radar clutter time series. The estimation of the parameters of the stable distribution from the real clutter data was achieved by methods based on fractional lower-order moments, as described in [32]. For the particular clutter series shown here, the characteristic exponent of the SαS distribution which best fits the data was calculated to be approximately $\alpha = 1.75$. To fit a Gaussian model, the variance was estimated by calculating the sample variance of the data. The impulsive nature of the clutter data is obvious in Figs. 1(a) and 2(b). Figs. 1(b) and 2(b) show that the SαS distribution

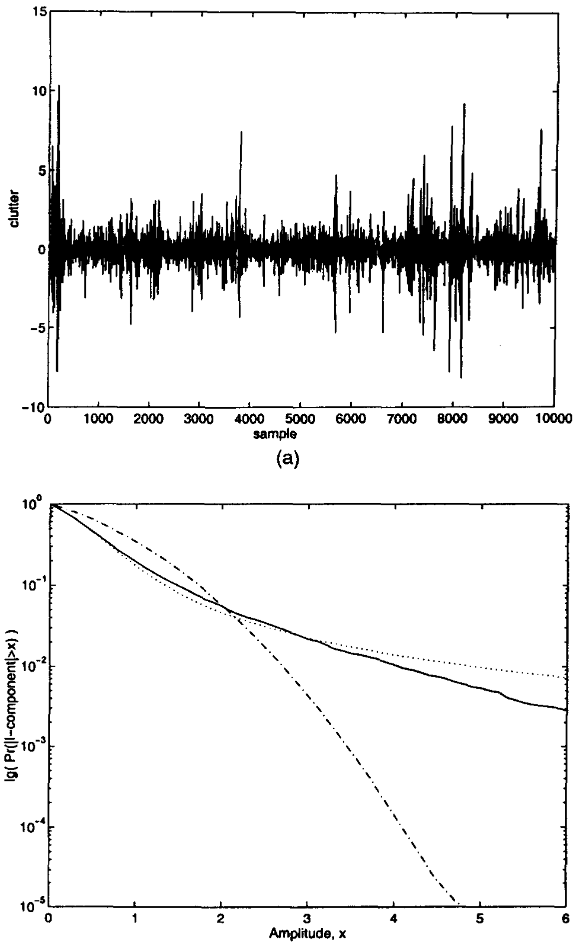

Fig. 1. (a) In-phase component of clutter time series. (b) Corresponding amplitude probability density curves. (Empirical: solid, SαS: dotted, Gaussian: dash-dotted).

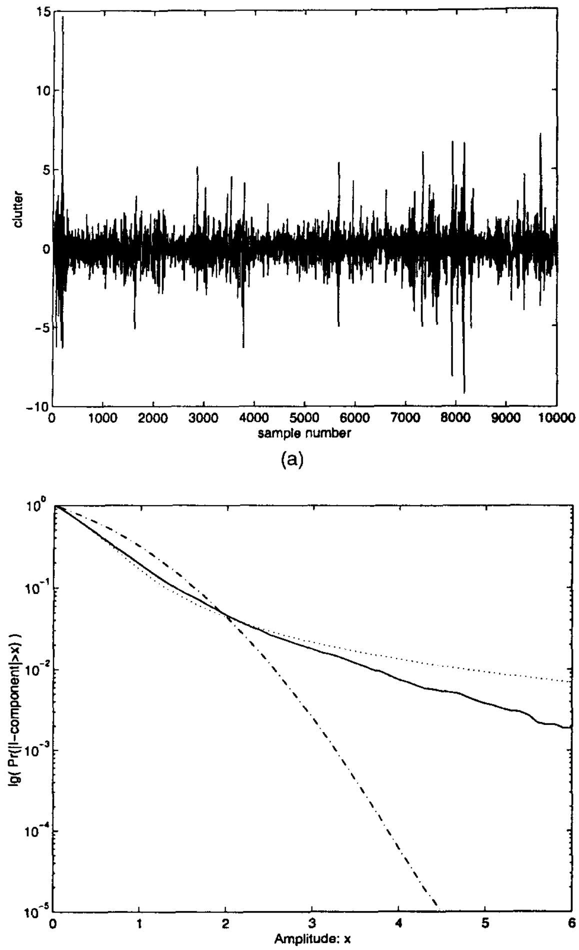

Fig. 2. (a) In-phase component of clutter time series. (b) Corresponding amplitude probability density curves. (Empirical: solid, SαS: dotted, Gaussian: dash-dotted).

fits the tails of the real data more accurately than the Gaussian density. Hence, it is demonstrated that the SαS distribution is superior to the Gaussian distribution for modeling the particular radar clutter data under study.

III. STAP PROBLEM FORMULATION

STAP refers to multidimensional adaptive algorithms that simultaneously combine the signals from the elements of an array antenna and the multiple pulses of a coherent radar waveform to suppress interference and provide target detection [17, 21].

Consider a uniformly spaced linear radar array antenna consisting of N elements, which transmits a coherent burst of M pulses at a constant pulse repetition frequency (PRF) $f_r = 1/T_r$ and over a certain range of directions of interest. The array receives signals generated by q narrowband moving targets which are located at azimuth angles $\{\phi_k;\ k = 1,\ldots,q\}$ and have relative velocities with respect to the radar $\{\nu_k;\ k = 1,\ldots,q\}$ corresponding to Doppler frequencies $\{f_k;\ k = 1,\ldots,q\}$. The azimuth angles $\{\phi_k;\ k = 1,\ldots,q\}$ and Doppler frequencies $\{f_k;\ k = 1,\ldots,q\}$ are unknown deterministic parameters that have to be estimated from the radar measurements. Since the signals are narrowband, the propagation delay across the array is much smaller than the reciprocal of the signal bandwidth, and it follows that, by using a complex envelop representation, the array output can be expressed as [17]

$$\mathbf{x}(t) = \mathbf{V}(\psi,\omega)\mathbf{s}(t) + \mathbf{n}(t). \tag{11}$$

The quantities appearing in (11) are defined as follows.

1) $\mathbf{x}(t) = [x_1(t),\ldots,x_{MN}(t)]^T$ is the array output vector (N: number of array elements, M: number of pulses, t may refer to the number of the coherent processing intervals (CPIs) available at the receiver).

2) $\mathbf{s}(t) = [\beta_1(t),\ldots,\beta_q(t)]^T$ is the signal vector emitted by the sources as received at the reference sensor 1 of the array. In this work, in formulating the ML function, we consider the signals as unknown, deterministic quantities that are nuisance parameters in the estimation problem, as opposed to the quantities of interest, i.e., the target angle and Doppler frequencies.

3) $\mathbf{V}(\psi,\omega) = [\mathbf{v}(\psi_1,\omega_1),\ldots,\mathbf{v}(\psi_q,\omega_q)]$ is the *space-time steering matrix* where $\psi_k = 2\pi(d/\lambda_0)\sin(\phi_k)$ is the normalized angle and $\omega_k = 2\pi(f_k/f_r)$ is the normalized Doppler.

4) $\mathbf{v}(\psi_k,\omega_k) = \mathbf{b}(\omega_k)\otimes\mathbf{a}(\psi_k)$ is the *space-time steering vector*, where $\otimes$ denotes the Kronecker matrix product, and

$-\mathbf{a}(\psi_k) = [1, e^{-j\psi_k},\ldots,e^{-j(N-1)\psi_k}]^T$ is the spatial steering vector

$-\mathbf{b}(\omega_k) = [1, e^{-j\omega_k},\ldots,e^{j(M-1)\omega_k}]^T$ is the temporal steering vector.

5) $\mathbf{n}(t) = [n_1(t),\ldots,n_{MN}(t)]^T$ is the noise vector.

The noise vector $\mathbf{n}$ (we drop the index t for notational convenience) encompasses components due to interference sources or jammers, clutter, and white thermal noise, respectively:

$$\mathbf{n} = \mathbf{n}_j + \mathbf{n}_c + \mathbf{n}_w. \tag{12}$$

The component $\mathbf{n}_w$ is due to the thermal noise present at the sensor elements and it is spatially and temporally white.

The jamming environment consists of several sources that are assumed to be temporally white (barrage jammers spread over all Doppler frequencies at a particular azimuth). Hence, jamming looks like thermal noise in the time domain, but like a discrete clutter source in the spatial domain. Then, the noise component due to a jammer located at (normalized) angle ψ_j is given by

$$\mathbf{n}_j = \mathbf{j}_j \otimes \mathbf{a}(\psi_j) \tag{13}$$

where $\mathbf{j}_j = [j_0, j_1, \ldots, j_{M-1}]^T$ is the $M \times 1$ random vector containing the jammer amplitudes and $\mathbf{a}(\psi_j)$ is the spatial steering vector in direction ψ_j.

Radar clutter is defined as the echoes from any scatterers considered to be not of a tactical significance. When considering a target at a given range, the clutter returns will come from all areas at a so-called *ambiguous range* R_i, corresponding to the range gate of interest. As an approximation to a continuous field of clutter, the clutter returns for each ambiguous range will be modeled as a superposition of a large number N_c of independent clutter sources that are evenly distributed in a circular ring about the radar platform. The location of the ikth clutter patch is described by its azimuth ϕ_k and ambiguous range R_i. Assuming that the normalized Doppler frequency of the ikth patch is ω_{ik}, the clutter component of the space-time snapshot is given by

$$\mathbf{n}_c = \sum_{i=1}^{N_r} \sum_{k=1}^{N_c} c_{ik} \mathbf{v}(\psi_{ik}, \omega_i k) \tag{14}$$

where c_{ik} is the random amplitude from the ikth clutter patch.

Assuming the availability of S CPIs $t_1, \ldots, t_S$, the data can be expressed as

$$\mathbf{X} = \mathbf{V}(\psi, \omega)\mathbf{S} + \mathbf{N} \tag{15}$$

where $\mathbf{X}$ and $\mathbf{N}$ are the $MN \times S$ matrices

$$\mathbf{X} = [\mathbf{x}(t_1), \ldots, \mathbf{x}(t_S)] \tag{16}$$

$$\mathbf{N} = [\mathbf{n}(t_1), \ldots, \mathbf{n}(t_S)] \tag{17}$$

and $\mathbf{S}$ is the $q \times S$ matrix

$$\mathbf{S} = [\mathbf{s}(t_1), \ldots, \mathbf{s}(t_S)]. \tag{18}$$

Our objective is to jointly estimate the directions-of-arrival $\{\phi_k;\ k = 1, \ldots, q\}$ and the Doppler frequencies $\{f_k;\ k = 1, \ldots, q\}$ of the source targets. More specifically, our goal here is twofold. First, we want to derive CRBs on the estimation accuracy of STAP processors when the noise components are of a heavy-tailed nature following the Cauchy probability density function. Then, we want to derive robust STAP processors for target parameter estimation in environments of heavy-tailed noise modeled as an alpha-stable process. In order to handle an analytically tractable problem and obtain insights to the estimation problem in impulsive noise backgrounds, in the following we assume that the noise components $\mathbf{n}(t)$ are uncorrelated both in the spatial (element-to-element) and temporal (pulse-to-pulse) domains. We acknowledge that this assumption is hardly ever met in practice, especially when considering clutter in the case of high PRF radars. As such, the results in this paper should be viewed as a first-order study on STAP methods and their corresponding bounds of performance in impulsive noise environments. To address the more general case of heavy-tailed correlated noise, the class of *multivariate sub-Gaussian* random processes can be used as a modeling tool, an approach that is currently pursued by the authors.

IV. JOINT TARGET ANGLE AND DOPPLER ML ESTIMATION IN CAUCHY NOISE

In this section, we study the problem of simultaneous target angle and Doppler estimation in severe noise environments. Throughout the rest of this work we assume the presence of *uncorrelated* additive impulsive noise at the radar array. We consider the case of additive complex isotropic Cauchy noise and derive the Cramér–Rao lower bounds on the estimation errors of any unbiased estimator of the target angle and Doppler.

For the purposes of this section, we assume that S snapshots for any target are available at the radar array processor. We arrange the received signals at time t in a $q \times q$ diagonal matrix $\beta(t)$:

$$\begin{aligned}\beta(t) &= \mathrm{diag}[\beta_1(t) \cdots \beta_q(t)] \\ &= \mathrm{diag}[\beta_{\Re,1}(t) \cdots \beta_{\Re,q}(t)] + j \cdot \mathrm{diag}[\beta_{\Im,1}(t) \cdots \beta_{\Im,q}(t)] \\ &= \beta_{\Re} + j \cdot \beta_{\Im} \qquad t = 1, \ldots, S\end{aligned} \tag{19}$$

where $\beta_{\Re,i}(t) = \Re\{\beta_i(t)\}$, $\beta_{\Im,i}(t) = \Im\{\beta_i(t)\}$, and $\Re\{\cdot\}$ and $\Im\{\cdot\}$ are the real and imaginary part operators, respectively. We assume that the noise present at the array sensors is modeled as a complex isotropic Cauchy process with probability density function given by

$$\chi_\gamma(r) = \frac{\gamma}{2\pi(r^2 + \gamma^2)^{3/2}}. \tag{20}$$

Under the assumption that the noise samples are statistically independent from one another both along the array sensors and along time, it follows that the joint density function of the sampled data is given by

$$\begin{aligned} f(\mathbf{X}) &= \prod_{t=1}^{S} \prod_{i=1}^{MN} \chi_\gamma \left(\left| x_i(t) - \sum_{k=1}^{q} \beta_k(t) v_i(\psi_k, \omega_k) \right| \right) \\ &= \frac{\gamma^{MNS}}{(2\pi)^{MNS} \prod_{t=1}^{S} \prod_{i=1}^{MN} (\gamma^2 + |x_i(t) - \sum_{k=1}^{q} \beta_k(t) v_i(\psi_k, \omega_k)|^2)^{3/2}} \end{aligned} \tag{21}$$

where $v_i(\psi_k, \omega_k)$ is the ith element of the space-time steering vector $\mathbf{v}(\psi_k, \omega_k)$. The estimation problem involves $2Sq + 2q + 1$ real valued parameters. We arrange them to form a $(2q(S+1)+1) \times 1$ parameter vector:

$$\eta = [\gamma \quad \beta_{\Re,1}(1)\cdots\beta_{\Re,q}(1) \quad \beta_{\Im,1}(1)\cdots\beta_{\Im,q}(1)\cdots\beta_{\Re,1}(S)\cdots \beta_{\Re,q}(S) \quad \beta_{\Im,1}(S)\cdots\beta_{\Im,q}(S) \quad \psi_1\cdots\psi_q \quad \omega_1\cdots\omega_q]^T. \tag{22}$$

The log likelihood function $L(\mathbf{X};\eta)$, ignoring the constant terms, is given by

$$L(\mathbf{X};\eta) = MNS\log\gamma - \frac{3}{2}\sum_{i=1}^{NM}\sum_{t=1}^{S} \times \log\left(\gamma^2 + \left|x_i(t) - \sum_{k=1}^{q}\beta_k(t)v_i(\psi_k,\omega_k)\right|^2\right). \tag{23}$$

The target amplitudes and noise dispersion are considered as unknown nuisance parameters that have to be estimated along with the target angles and Doppler frequencies. An iterative procedure based on the gradient descent principle can be applied in order to solve for the parameters of interest η. In general, the cost function described in (23) is nonconvex and the optimization procedure has to be initialized sufficiently close to the global extremum. Monte-Carlo simulation results on the estimation accuracy of the ML technique are shown in Section VI. Due first to the computational complexity associated with the multivariate nonlinear optimization problem involved with the solution of (23) and second, to the initialization problems related to the ML formulation, suboptimal subspace-based parameter estimators are developed in Section V for the STAP problem under study. But first, the next section presents the CRBs on the target angle and Doppler estimation errors for the additive Cauchy interference scenario to assess the best-case estimation accuracy which can be achieved for this type of additive noise.

A. Cramér–Rao Bound for Cauchy Noise

The CRB for the error variance of an unbiased estimator $\hat{\Theta}$ of a vector of unknown deterministic parameters Θ satisfies [33]:

$$\mathbf{C}_{\hat{\Theta}} - \mathbf{J}^{-1}(\Theta) \geq 0 \tag{24}$$

where $\mathbf{C}_{\hat{\Theta}}$ is the covariance matrix of $\hat{\Theta}$, $\mathbf{J}(\Theta)$ is the Fisher information matrix, and $\mathbf{T} \geq 0$ is interpreted as meaning that the matrix $\mathbf{T}$ is semidefinite positive. Then, the following theorem holds for the case of complex isotropic Cauchy noise.

THEOREM 1 *The CRB for ψ, ω, and γ is given by*

$$\mathrm{CRB}(\psi,\omega) = \left[\sum_{t=1}^{S}(\Sigma - \Upsilon^T(t)\Xi\Upsilon(t))\right]^{-1} \tag{25}$$

and

$$\mathrm{CRB}(\gamma) = \frac{5}{4}\frac{\gamma^2}{MNS} \tag{26}$$

where

$$\Sigma = \frac{3}{5\gamma^2}\cdot\begin{bmatrix} \Re\left\{\sum_{t=1}^{S}\beta^H(t)\mathbf{D}^H_{b\otimes d_a}\mathbf{D}_{b\otimes a}\beta(t)\right\} & \Re\left\{\sum_{t=1}^{S}\beta^H(t)\mathbf{D}^H_{b\otimes d_a}\mathbf{D}_{d_b\otimes a}\beta(t)\right\} \\ \left[\Re\left\{\sum_{t=1}^{S}\beta^H(t)\mathbf{D}^H_{b\otimes d_a}\mathbf{D}_{d_b\otimes a}\beta(t)\right\}\right]^T & \Re\left\{\sum_{t=1}^{S}\beta^H(t)\mathbf{D}^H_{d_b\otimes a}\mathbf{D}_{b\otimes a}\beta(t)\right\} \end{bmatrix} \tag{27}$$

$$\Upsilon(t) = \frac{3}{5\gamma^2}\cdot\begin{bmatrix} \Re\{\beta^H(t)\mathbf{D}^H_{b\otimes d_a}\mathbf{D}_{b\otimes a}\} & \Im\{\beta^H(t)\mathbf{D}^H_{b\otimes d_a}\mathbf{D}_{b\otimes a}\} \\ \Re\{\beta^H(t)\mathbf{D}^H_{d_b\otimes a}\mathbf{D}_{b\otimes a}\} & \Im\{\beta^H(t)\mathbf{D}^H_{d_b\otimes a}\mathbf{D}_{b\otimes a}\} \end{bmatrix} \qquad t = 1,\ldots,S \tag{28}$$

$$\Xi = \frac{5\gamma^2}{3}\cdot\begin{bmatrix} [\Re\{\mathbf{D}^H_{b\otimes a}\mathbf{D}_{b\otimes a}\}]^{-1} & [\Im\{\mathbf{D}^H_{b\otimes a}\mathbf{D}_{b\otimes a}\}]^{-1} \\ -[\Re\{\mathbf{D}^H_{b\otimes a}\mathbf{D}_{b\otimes a}\}]^{-1} & [\Re\{\mathbf{D}^H_{b\otimes a}\mathbf{D}_{b\otimes a}\}]^{-1} \end{bmatrix} \tag{29}$$

and

$$\mathbf{D}_{b\otimes a} = [\mathbf{b}(\omega_1)\otimes\mathbf{a}(\psi_1),\ldots,\mathbf{b}(\omega_q)\otimes\mathbf{a}(\psi_q)] \tag{30}$$

$$\mathbf{D}_{d_b\otimes a} = [\mathbf{d}_b(\omega_1)\otimes\mathbf{a}(\psi_1),\ldots,\mathbf{d}_b(\omega_q)\otimes\mathbf{a}(\psi_q)] \tag{31}$$

$$\mathbf{D}_{b\otimes d_a} = [\mathbf{b}(\omega_1)\otimes\mathbf{d}_a(\psi_1),\ldots,\mathbf{b}(\omega_q)\otimes\mathbf{d}_a(\psi_q)] \tag{32}$$

where

$$\mathbf{d}_a(\psi_j) = [d_1^a(\psi_j)\cdots d_N^a(\psi_j)] = \left[\frac{\partial a_1(\psi_j)}{\partial\psi_j}\cdots\frac{\partial a_N(\psi_j)}{\partial\psi_j}\right],$$

$$\mathbf{d}_b(\omega_j) = [d_1^b(\omega_j)\cdots d_M^b(\omega_j)] = \left[\frac{\partial b_1(\omega_j)}{\partial\omega_j}\cdots\frac{\partial b_M(\omega_j)}{\partial\omega_j}\right]$$

and $\beta(t)$ is given by (19).

PROOF See Appendix A.

We should note that the above bound can be achieved only when there exist unbiased estimators for all the models parameters γ, $\beta(t)$, ψ, and ω. A useful insight on the CRB can be gained if we consider the case of a single target ($q = 1$) located in $\psi = (2\pi d/\lambda_0)\sin\phi$, with normalized Doppler shift $\omega = 2\pi f T_r$ and constant target amplitude β. In this case, we have

$$\mathrm{CRB}(\phi) = \frac{\gamma^2}{S|\beta|^2}\frac{\lambda_0^2}{(2\pi d)^2}\cdot\frac{5N(\|\mathbf{d}_b\|^2 - \delta_b^2/M)}{3\xi}\cdot\frac{1}{\cos^2(\phi)} \tag{33}$$

$$\mathrm{CRB}(f) = \frac{\gamma^2}{S|\beta|^2}\frac{1}{(2\pi T_r)^2}\cdot\frac{5M(\|\mathbf{d}_a\|^2 - \delta_a^2/N)}{3\xi} \tag{34}$$

where

$$\delta_a = \sum_{i=1}^{N}|d_i^a| \tag{35}$$

$$\delta_b = \sum_{i=1}^{M}|d_i^b| \tag{36}$$

$$\rho = \sum_{i=1}^{MN}|d_{g(i)}^a|\,|d_{f(i)}^b| \tag{37}$$

and

$$\xi = \left(M\|\mathbf{d}_a\|^2 - \frac{M}{N}\delta_a^2\right)\left(N\|\mathbf{d}_b\|^2 - \frac{N}{M}\delta_b^2\right) - (\delta_a\delta_b - \rho)^2. \tag{38}$$

As can be seen in (33) and (34), target angle accuracy is a function of Doppler frequency and vice versa. Finally, if we consider an airborne radar system that utilizes a uniform linear array antenna and a waveform with a uniform pulse repetition interval, the bounds (33) and (34) are given by

$$\mathrm{CRB}(\phi) = \frac{\gamma^2}{S|\beta|^2}\cdot\frac{\lambda_0^2}{(2\pi d)^2}\cdot\frac{20}{M^2N^2(N^2-1)}\cdot\frac{1}{\cos^2(\phi)} \tag{39}$$

and

$$\mathrm{CRB}(f) = \frac{\gamma^2}{S|\beta|^2}\cdot\frac{1}{(2\pi T_r)^2}\cdot\frac{20}{N^2M^2(M^2-1)}. \tag{40}$$

Hence, for a uniform linear array antenna employing a waveform with a uniform pulse repetition interval in an uncorrelated Cauchy noise environment, the CRBs for the variances of the target angle and Doppler estimates are independent of the target Doppler and angle, respectively. Naturally, in general the bounds are functions of the generalized signal-to-noise ratio (GSNR) function given by $S|\beta|^2/\gamma^2$, similarly to the Gaussian case where the bounds are functions of the signal-to-noise ratio (SNR). The larger the dispersion γ of the noise, the higher the CRB.

V. ARRAY COVARIATION MATRIX

The ML techniques, although asymptotically optimal (under certain regularity conditions they achieve the CRB), they are regarded as exceedingly complex due to the high computational load of the multivariate nonlinear optimization problem involved in the solution of (23) [34]. Hence, suboptimal methods need to be developed for the solution of the joint target angle and Doppler estimation problem for STAP applications in the presence of impulsive noise, when reduced computational cost is a crucial design requirement.

In this section, we assume that the q signal waveforms are noncoherent, statistically independent, complex isotropic SαS ($1 < \alpha \le 2$) random processes with zero location parameter and covariation matrix $\boldsymbol{\Gamma}_S = \mathrm{diag}(\gamma_{\beta_1},\ldots,\gamma_{\beta_q})$. Also, the noise vector $\mathbf{n}(t)$ is a complex isotropic SαS random process with the same characteristic exponent α as the signals. The noise is assumed to be independent of the signals with covariation matrix $\boldsymbol{\Gamma}_N = \gamma_n\mathbf{I}$.

Equation (11) can be written as

$$\mathbf{x}(t) = \mathbf{w}(t) + \mathbf{n}(t) \tag{41}$$

where $\mathbf{w}(t) = \mathbf{V}(\psi,\omega)\mathbf{s}(t)$. By the stability property, it follows that $\mathbf{w}(t)$ is also a complex isotropic SαS random vector with components

$$\begin{aligned} w_i(t) &= \mathbf{V}_i(\psi,\omega)\mathbf{s}(t) \\ &= v_i(\psi_1,\omega_1)\beta_1(t) + \cdots + v_i(\psi_q,\omega_q)\beta_q(t) \\ &\qquad i = 1,\ldots,MN. \end{aligned} \tag{42}$$

Also, it holds that $\mathbf{w}(t)$ is independent of $\mathbf{n}(t)$.

Now, we define the *covariation matrix*, $\boldsymbol{\Gamma}_X$, of the observation vector process $\mathbf{x}(t)$ as the matrix whose elements are the covariations $[x_i(t),x_j(t)]_\alpha$ of the components of $\mathbf{x}(t)$. We have that

$$\begin{aligned} [x_i(t),x_j(t)]_\alpha &= [w_i(t)+n_i(t), w_j(t)+n_j(t)]_\alpha \\ &= [w_i(t),w_j(t)]_\alpha + [w_i(t),n_j(t)]_\alpha \\ &\quad + [n_i(t),w_j(t)]_\alpha + [n_i(t),n_j(t)]_\alpha. \end{aligned} \tag{43}$$

By the independence assumption of $\mathbf{w}(t)$ and $\mathbf{n}(t)$ and by property P3 we have that

$$[w_i(t),n_j(t)]_\alpha = 0 \tag{44}$$

and

$$[n_i(t),w_j(t)]_\alpha = 0. \tag{45}$$

Also, by using (42) and properties P1 and P2 it follows that

$$\begin{aligned} [w_i(t),w_j(t)]_\alpha &= \left[\sum_{k=1}^{q} v_i(\psi_k,\omega_k)\beta_k(t), w_j(t)\right]_\alpha \\ &= \sum_{k=1}^{q} v_i(\psi_k,\omega_k)[\beta_k(t),w_j(t)]_\alpha \\ &= \sum_{k=1}^{q} v_i(\psi_k,\omega_k)\left[\beta_k(t), \sum_{l=1}^{q} v_j(\psi_l,\omega_l)\beta_l(t)\right]_\alpha \\ &= \sum_{k=1}^{q} v_i(\psi_k,\omega_k)v_j^{\langle\alpha-1\rangle}(\psi_k,\omega_k)\gamma_{\beta_k} \end{aligned} \tag{46}$$

where $\gamma_{\beta_k} = [\beta_k, \beta_k]_\alpha$. Finally, due to the noise assumption made earlier, it holds that

$$[n_i(t), n_j(t)]_\alpha = \gamma_n \delta_{i,j} \tag{47}$$

where $\delta_{i,j}$ is the Kronecker delta function. Combining (43)–(47) we obtain the following expression for the covariations of the sensor measurements:

$$[x_i(t), x_j(t)]_\alpha = \sum_{k=1}^{q} v_i(\psi_k, \omega_k) v_j^{\langle\alpha-1\rangle}(\psi_k, \omega_k)\gamma_{\beta_k} + \gamma_n \delta_{i,j} \qquad i,j = 1,\ldots,MN. \tag{48}$$

In addition, the dispersion and covariation coefficients of the array sensor measurements are given, respectively, by

$$\gamma_{x_j(t)} = \sum_{k=1}^{q} |v_j(\psi_k, \omega_k)|^\alpha \gamma_{\beta_k} + \gamma_n \qquad j = 1,\ldots,MN \tag{49}$$

and

$$\lambda_{x_i(t),x_j(t)} = \frac{\sum_{k=1}^{q} v_i(\psi_k, \omega_k) v_j^{\langle\alpha-1\rangle}(\psi_k, \omega_k)\gamma_{\beta_k} + \gamma_n \delta_{i,j}}{\sum_{k=1}^{q} |v_j(\psi_k, \omega_k)|^\alpha \gamma_{\beta_k} + \gamma_n} \qquad i,j = 1,\ldots,MN. \tag{50}$$

In matrix form, (48) gives the following expression for the covariation matrix of the observation vector:

$$\Gamma_X \stackrel{\Delta}{=} [\mathbf{x}(t), \mathbf{x}(t)]_\alpha = \mathbf{V}(\psi, \omega)\Gamma_S \mathbf{V}^{\langle\alpha-1\rangle}(\psi, \omega) + \gamma_n \mathbf{I} \tag{51}$$

where the (i,j)th element of matrix $\mathbf{V}^{\langle\alpha-1\rangle}(\psi,\omega)$ results from the (j,i)th element of $\mathbf{V}(\psi,\omega)$ according to the operation

$$\begin{aligned}[\mathbf{V}^{\langle\alpha-1\rangle}(\psi,\omega)]_{i,j} &= [\mathbf{V}(\psi,\omega)]_{j,i}^{\langle\alpha-1\rangle} \\ &= |[\mathbf{V}(\psi,\omega)]_{j,i}|^{\alpha-2}[\mathbf{V}(\psi,\omega)]_{j,i}^{*}.\end{aligned} \tag{52}$$

Clearly, when $\alpha = 2$, i.e., for Gaussian distributed signals and noise, the expression for the covariation matrix is identical to the well-known expression for the covariance matrix:

$$\mathbf{R}_X = \mathbf{V}(\psi,\omega)\Sigma \mathbf{V}^H(\psi,\omega) + \sigma^2 \mathbf{I} \tag{53}$$

where Σ is the signal covariance matrix.

The space-time steering vectors $\mathbf{v}(\psi_k, \omega_k)$ comprising matrix $\mathbf{V}(\psi)$ are the Kronecker products of two *Vandermonde* vectors, namely the spatial steering vector $\mathbf{a}(\psi_k)$ and the temporal steering vector $\mathbf{b}(\omega_k)$. Hence, the magnitude of any component of the space-time steering vector is equal to unity and the term $|[\mathbf{V}(\psi,\omega)]_{j,i}|^{\alpha-2}$ in (52) is equal to one. Therefore, (52) results into

$$[\mathbf{V}^{\langle\alpha-1\rangle}(\psi,\omega)]_{i,j} = [\mathbf{V}(\psi,\omega)]_{j,i}^{*} \tag{54}$$

and thus the covariation matrix can be written as

$$\Gamma_X = \mathbf{V}(\psi,\omega)\Gamma_S \mathbf{V}^H(\psi,\omega) + \gamma_n \mathbf{I}. \tag{55}$$

Also, from (49) and (50) the dispersion and covariation coefficients of the array sensor measurements can be written as

$$\gamma_{x_j(t)} = \sum_{k=1}^{q} \gamma_{\beta_k} + \gamma_n \qquad j = 1,\ldots,MN \tag{56}$$

and

$$\lambda_{x_i(t),x_j(t)} = \frac{\sum_{k=1}^{q} v_i(\psi_k, \omega_k) v_j^{*}(\psi_k, \omega_k)\gamma_{\beta_k} + \gamma_n \delta_{i,j}}{\sum_{k=1}^{q} \gamma_{\beta_k} + \gamma_n} \qquad i,j = 1,\ldots,MN. \tag{57}$$

Observing (55), we conclude that standard subspace techniques can be applied to the covariation or the covariation coefficient matrices of the observation vector to extract the bearing information. More specifically, it follows that the rank of matrix $\mathbf{V}(\psi,\omega)\Gamma_S \mathbf{V}^H(\psi,\omega)$ is q, with the smallest $(MN - q)$ of its eigenvalues equal to zero. In other words, if we let $\rho_1 \geq \rho_2 \geq \cdots \geq \rho_{MN}$ denote the eigenvalues of matrix Γ_X, then

$$\rho_{q+1} = \cdots = \rho_{MN} = \gamma_n. \tag{58}$$

In practice, we have to estimate the covariation matrix from a finite number of array sensor measurements. A proposed estimator for the covariation coefficient $\lambda_{x_i(t),x_j(t)}$ is called the *fractional lower order (FLOM) estimator* and is given by [35]

$$\hat{\lambda}_{x_i(t),x_j(t)} = \frac{\sum_{t=1}^{n} x_i(t) x_j^{\langle p-1\rangle}(t)}{\sum_{t=1}^{n} |x_j(t)|^p} \tag{59}$$

for some $0 \leq p < \alpha$. The influence of the parameter p to the performance of the FLOM estimator for the covariation coefficient is studied in [23]. It is shown that for the case of non-Gaussian stable signals $(1 < \alpha < 2)$, values of p in the range $(1/2, \alpha/2)$ result into estimators with the smallest standard deviations. Naturally, for Gaussian signals the optimal value of p is 2 and the resulting FLOM estimator is simply the least-squares estimator, as expected.

We refer to the new algorithm resulting from the eigendecomposition of the array covariation coefficient matrix as the **2-D robust covariation-based MUSIC** or **2-D ROC-MUSIC**. By denoting the corresponding eigenvectors of Γ_X by $\{\mathbf{u}_i\}_{i=1}^{MN}$, the 2-D ROC-MUSIC spectrum can be expressed as

$$S_{\text{2-D ROC-MUSIC}}(\psi,\omega) = \frac{1}{\sum_{i=q+1}^{MN} |\mathbf{v}^H(\psi,\omega)\mathbf{u}_i|^2}. \tag{60}$$

The locations of the targets in angle and Doppler are determined by the values of (ψ,ω) for which the spectrum given by (60) peaks.

VI. SIMULATION EXPERIMENTS

In this section, two sets of experiments are performed to demonstrate the theoretical results on the joint target angle and Doppler estimation in alpha-stable impulsive interference. First, we compare the ML estimator based on the Cauchy noise assumption (MLC) with the ML estimator based on the Gaussian noise assumption (MLG) and study their estimation accuracy as a function of three parameters, namely the number of snapshots S, the noise dispersion γ, and the noise characteristic exponent α. Then, we demonstrate the improved resolution capability of the 2-D ROC-MUSIC versus the 2-D MUSIC as a function of the noise characteristic exponent α and target separation.

Our study in this work concentrates on the estimation accuracy and resolution capabilities of the proposed methods. Clearly, important practical aspects involve the initialization of the ML-based methods and the computational requirements for obtaining the target parameter estimates using ML or subspace-based methods. We briefly discuss the initialization issue related with the ML algorithms later in this section. The computational complexity of the ML methods versus that of the subspace-based methods has been studied by Ottersten, et al. [34]. The computational load of the ML-based methods depends on the numerical method used to optimize the cost function. The associated number of iterations to achieve convergence depends on the initialization of the parameters and on the step-size parameter. On the other hand, the computational cost of the subspace-based methods is dominated by the formation of the sample covariance or covariation matrices and the calculation of the required eigendecomposition. To reduce this cost, the special matrix structure may be used, as discussed in [34].

In all the experiments, the radar array is linear with five sensors spaced half wavelength apart ($N = 5$). The number of transmitted pulses is $M = 10$. We model the complex amplitudes of the target returns $\beta_i(t)$ as complex Gaussian RVs whose variance is determined by the desired signal power. In every experiment we perform 500 Monte-Carlo runs to compute the mean square error (MSE) of the estimates and the resolution probabilities.

A. Estimation Accuracy of the ML Methods

In this example, we study the estimation accuracy of MLC and MLG as a function of three parameters, namely the number of snapshots S, the noise dispersion γ, and the characteristic exponent α. The optimization for the MLC and MLG methods is performed by a steepest descent algorithm with variable stepsize selected by means of Armijo's rule [36]. Because this set of simulations studies the estimation accuracy of the ML algorithms (i.e., how close, in terms of MSE, is the global minimum of the cost functions to the true parameters), the initial conditions were chosen to be close to the true target angle and Doppler values. In other words, we were making sure that the algorithms converged to the global minimum [34].

Since the alpha-stable family for $\alpha < 2$ determines processes with infinite variance, we define an alternative input SNR. Namely, we define the input GSNR to be the ratio of the signal power over the noise dispersion γ:

$$\mathrm{GSNR} = 10\log_{10}\left(\frac{1}{\gamma S}\sum_{t=1}^{S}|\beta(t)|^2\right). \tag{61}$$

As shown in (61), the input GSNR is defined on a single element for a single pulse and averaged over the snapshots.

1) *Number of Snapshots S*: In the first experiment, we study the influence of the number of snapshots S to the performance of the algorithms. The noise follows the complex isotropic Cauchy distribution with dispersion $\gamma = 10$. For this experiment, the GSNR is kept constant at 7 dB.

Figs. 3(a) and (b) show the resulting MSE of the angle and Doppler estimators, respectively, as a function of the number of snapshots. The CRB is also plotted. As expected, the MLC estimator has the best performance since it is the optimal estimator for this type of noise. Also, the complete failure of the MLG processor for this type of impulsive noise is apparent. We can see that the MSE of the MLG estimator does not decrease as the number of snapshots increases. This is because the more snapshots are available at the radar array, the larger the probability that more impulsive noise samples are incorporated into the data.

2) *Noise Dispersion γ*: In this experiment, we study the influence of the noise dispersion γ, i.e., the influence of the GSNR to the performance of the methods. Fig. 4 shows the resulting MSE of the estimated angle and Doppler as a function of the GSNR. The CRB is also plotted. The number of snapshots available to the algorithm is $S = 10$. Again, the MLC has the best performance. Naturally, the larger the GSNR, the smaller the MSE of the MLC method.

3) *Characteristic Exponent α*: The importance of the last experiment rests in its study of the robustness of the algorithms in different environments. Of course, the MLG estimator is asymptotically optimal for additive Gaussian noise ($\alpha = 2$), and the introduced MLC estimator is asymptotically optimal for additive Cauchy noise ($\alpha = 1$). Here, we test the performance of the estimators in a wide range of noise environments, i.e., when the characteristic exponent, α, of the noise stable law is changing.

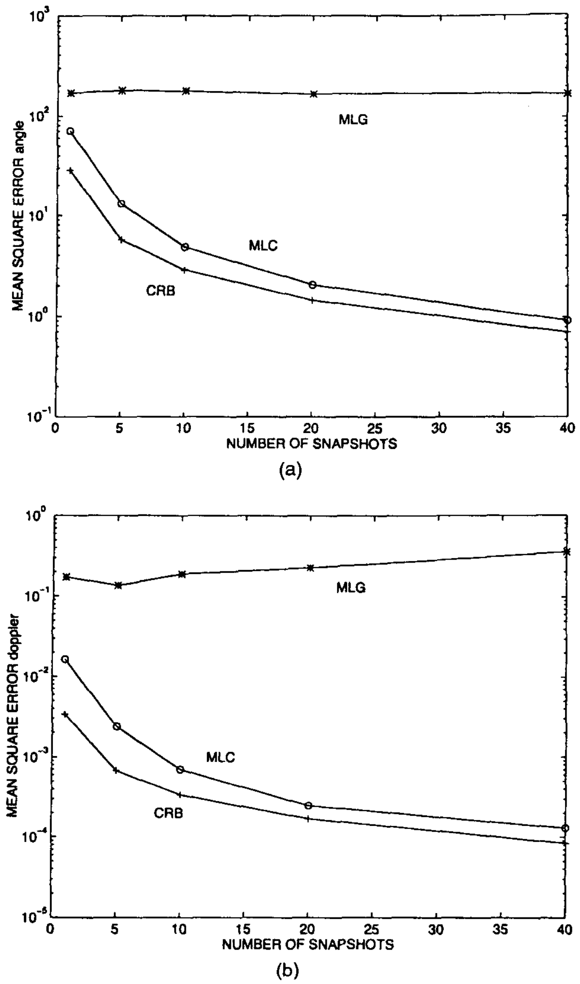

Fig. 3. MSE of estimated angle (a) and Doppler (b) curves, and CRB as function of number of snapshots S.

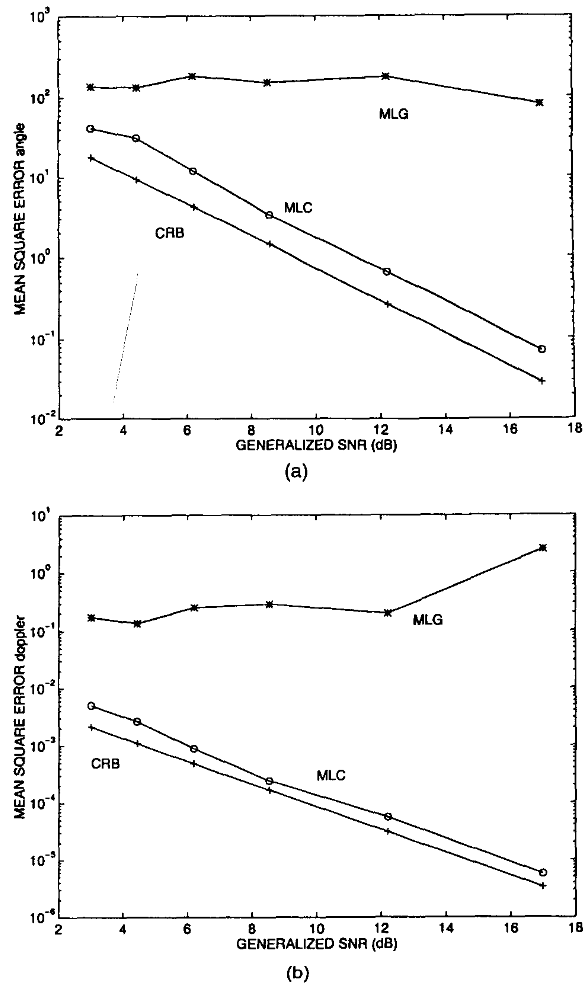

Fig. 4. MSE estimated angle (a) and Doppler (b) curves, and CRB as function of GSNR.

Fig. 5 shows the resulting MSE curves as functions of the characteristic exponent α. The GSNR is 7 dB and the number of snapshots available to the algorithm is $S = 10$. As we can see, the Cauchy estimator is practically insensitive to the changes of α. On the other hand, the MLG algorithm exhibits very large mean square estimation errors for non-Gaussian environments. Note that when $\alpha = 2$, i.e., for the Gaussian noise case, the MLG method has the least MSE, as expected. These observations, combined with the fact that the ML method based on the Cauchy assumption has computational complexity similar to the ML method based on the Gaussian assumption, justify the importance of the Cauchy estimator for the STAP problem in practice.

B. Performance Comparison between 2-D MUSIC and 2-D ROC MUSIC

In this section, we show results on the resolution capability of 2-D ROC-MUSIC versus 2-D MUSIC as functions of the noise characteristic exponent α. Three moving targets impinge on the array from directions $\Phi = [-20°, -40°, 40°]$ and they have normalized Doppler values $\Omega = [-0.3, -0.2, 0.3]$). The number of snapshots available to the algorithms is $S = 1000$. The noise follows the bivariate isotropic stable distribution. The GSNR is 22.3 dB. The characteristic exponent α of the additive noise is unknown to the 2-D ROC-MUSIC algorithm. The parameter p in the estimation of the covariation matrix (see (59)) was set equal to $p = 0.8$. Clearly, 2-D MUSIC can be thought as a special case of 2-D ROC-MUSIC with $p = 2$.

In Figs. 6 and 7, isosurfaces of space-time spectral estimates are shown for the 2-D ROC-MUSIC and 2-D MUSIC algorithms. Two types of alpha-stable noise corresponding to two values of the characteristic exponent $\alpha = 1.5$ and $\alpha = 2.0$ (Gaussian) were used. We can see that the 2-D MUSIC method exhibits high-resolution performance only for the case of additive Gaussian noise while it does not

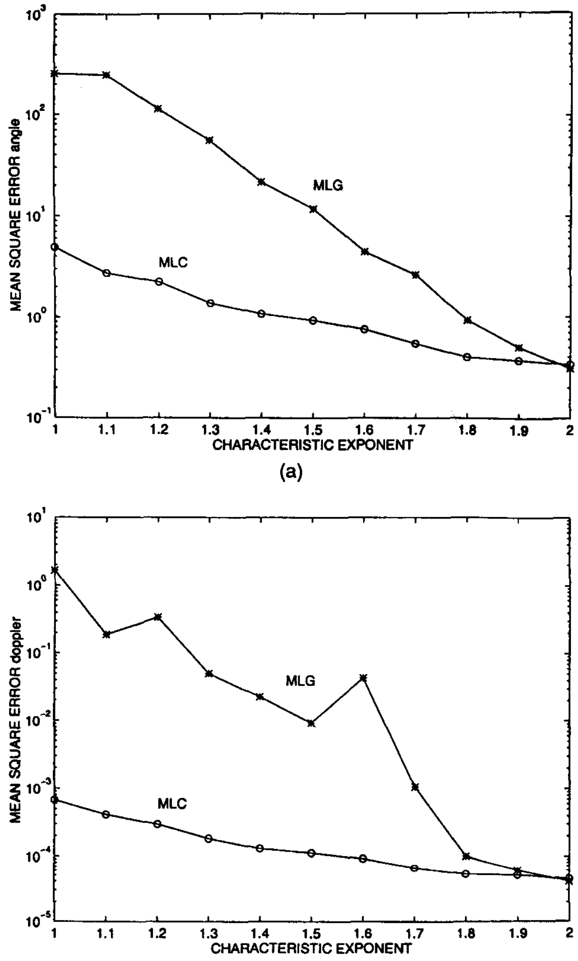

Fig. 5. MSE of estimated angle (a) and Doppler (b) curves as function of characteristic exponent α.

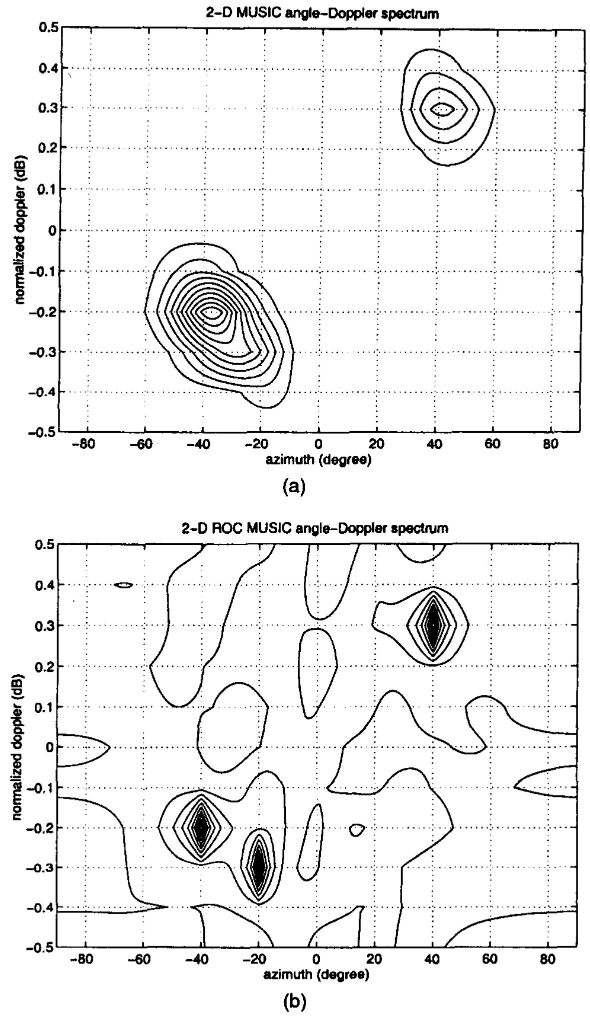

Fig. 6. 2-D MUSIC (a) and 2-D ROC-MUSIC (b) angle-Doppler spectra ($N = 5, M = 10, \Phi = [-20°, -40°, 40°]$, $\Omega = [-0.3, -0.2, 0.3]$). Additive stable noise ($\alpha = 1.5$).

resolve the two closely moving targets when the additive noise is stable with $\alpha = 1.5$. On the other hand, the 2-D ROC-MUSIC method exhibits better resolution capabilities for non-Gaussian additive noise environments ($\alpha = 1.5$) and at the same time, performs well for Gaussian interference. Fig. 8(a) depicts the improved performance of the 2-D ROC-MUSIC over that of 2-D MUSIC in terms of resolution probability, for values of α in the range $(1,2)$. The results are based on 500 independent Monte-Carlo runs.

Fig. 8(b) illustrates the variation of the algorithmic performance with respect to the spatial angle separation of the two closely spaced incoming targets for GSNR = 22.3 dB, ($\alpha = 1.5$). As expected, the resolution capability of both algorithms improves with increased angle separation between the two targets. But for a given probability of resolution, the 2-D ROC-MUSIC algorithm requires a lower angle separation threshold than the 2-D MUSIC algorithm.

VII. CONCLUDING REMARKS

We considered the problem of target-angle and Doppler estimation with an airborne radar employing STAP. We derived CRBs on angle and Doppler estimator accuracy for the case of additive Cauchy interference. We introduced a new joint spatial- and Doppler-frequency high-resolution estimation technique based on the fractional lower order statistics of the measurements of a radar array. We showed that the proposed 2-D ROC-MUSIC algorithm provides better angle/Doppler estimates than the 2-D MUSIC in a wide range of impulsive uncorrelated interference environments and can be used in STAP radar applications.

This paper assumed that the additive impulsive noise present at the STAP radar array is both spatially and temporally white. In most practical situations, this is hardly the case. Hence, current research

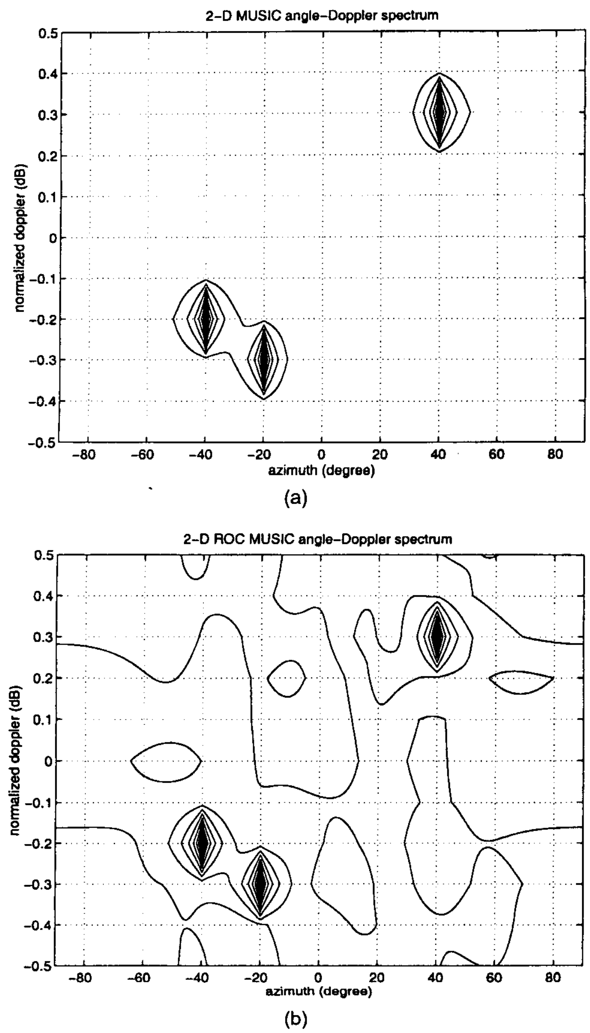

Fig. 7. 2-D MUSIC (a) and 2-D ROC-MUSIC (b) angle-Doppler spectra ($N = 5, M = 10, \Phi = [-20°, -40°, 40°]$, $\Omega = [-0.3, -0.2, 0.3]$). Additive stable noise ($\alpha = 2.0$).

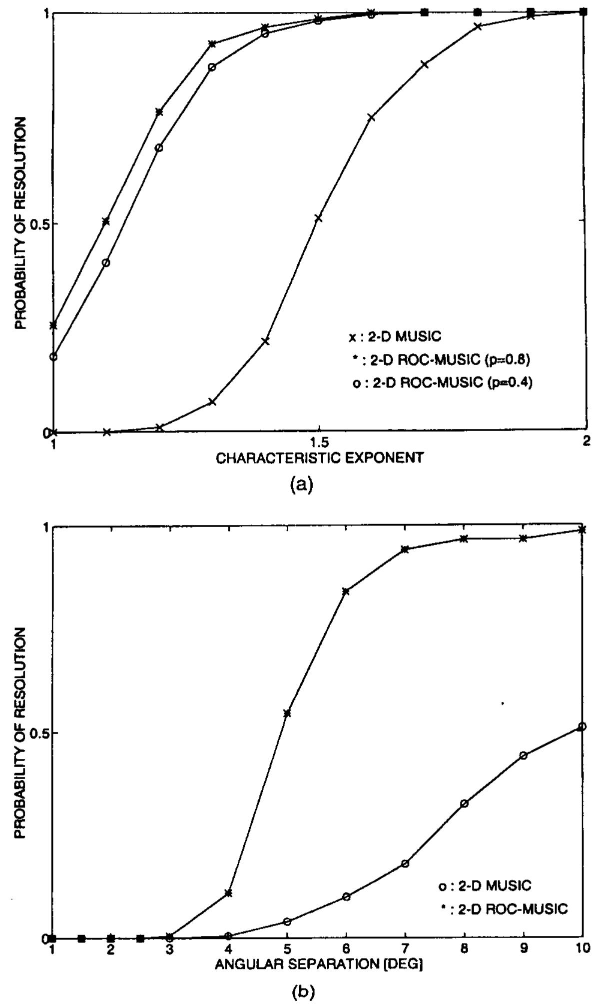

Fig. 8. Probability of resolution as function of characteristic exponent α (a) and source angular separation ($\alpha = 1.5$) (b).

includes the study of methods for STAP parameter estimation in the presence of *correlated impulsive noise backgrounds*. Towards this goal, the theory of *multivariate sub-Gaussian* random processes provides an elegant and mathematically tractable framework for the solution of the detection and parameter estimation problems in the presence of impulsive correlated radar clutter. This research is currently underway and results will be announced soon.

APPENDIX A. DERIVATION OF CRB FOR COMPLEX ISOTROPIC CAUCHY NOISE

In this Appendix, we derive the CRB for the most general case of multiple targets in the presence of complex isotropic Cauchy noise of unknown dispersion parameter γ. In the following, we extensively use the following proposition [22] about the magnitude r and phase φ of the noise.

PROPOSITION 1 *The amplitude r and phase φ of the noise following the complex isotropic Cauchy distribution are independent, the noise phase φ is uniformly distribuited in $[0, 2\pi]$ and the magnitude r satisfies*

$$\mathcal{E}\left\{\frac{r^2}{(\gamma^2 + r^2)^2}\right\} = \frac{2}{15\gamma^2}. \tag{62}$$

Now, we proceed by proving Theorem 1. Let η represent the $(2Sq + 2q + 1)$-dimensional vector of unknown parameters

$$\eta = [\gamma \quad \beta_{\Re,1}(1)\cdots\beta_{\Re,q}(1) \quad \beta_{\Im,1}(1)\cdots\beta_{\Im,q}(1)\cdots\beta_{\Re,1}(S)\cdots \beta_{\Re,q}(S) \quad \beta_{\Im,1}(S)\cdots\beta_{\Im,q}(S) \quad \psi_1\cdots\psi_q \quad \omega_1\cdots\omega_q]^T. \tag{63}$$

The *Fisher Information Matrix* is given by

$$\mathbf{J}(\eta) = \mathcal{E}\left\{\left(\frac{\partial L(\eta)}{\partial \eta}\right)\left(\frac{\partial L(\eta)}{\partial \eta}\right)^T\right\}. \tag{64}$$

First, we calculate the derivatives of the log-likelihood function given in (23)

$$\frac{\partial L}{\partial \gamma} = \frac{MNS}{\gamma} - \frac{3}{2}\sum_{t=1}^{S}\sum_{i=1}^{MN}\frac{\gamma}{\gamma^2 + |n_i(t)|^2} \tag{65}$$

$$\frac{\partial L}{\partial \psi_j} = 3\sum_{t=1}^{S}\sum_{i=1}^{MN}\frac{\Re\{\beta_j^*(t)b_{f(i)}^*(\omega_j)(d_{g(i)}^a(\psi_j))^* n_i(t)\}}{\gamma^2 + |n_i(t)|^2}$$

$$j = 1,\ldots,q \tag{66}$$

$$\frac{\partial L}{\partial \omega_j} = 3\sum_{t=1}^{S}\sum_{i=1}^{MN}\frac{\Re\{\beta_j^*(t)a_{g(i)}^*(\psi_j)(d_{f(i)}^b(\omega_j))^* n_i(t)\}}{\gamma^2 + |n_i(t)|^2}$$

$$j = 1,\ldots,q \tag{67}$$

where $0 \le f(i) \le M$ and $0 \le g(i) \le N$ are such that $b_{f(i)} \cdot a_{g(i)} = (\mathbf{b} \otimes \mathbf{a})_i$;

$$\frac{\partial L}{\partial \beta_{\Re,j}(t)} = 3\sum_{i=1}^{MN}\frac{\Re[a_{g(i)}^*(\psi_j)b_{f(i)}^*(\omega_j)n_i(t)]}{\gamma^2 + |n_i(t)|^2}$$

$$j = 1,\ldots,q, \quad t = 1,\ldots,S \tag{68}$$

and

$$\frac{\partial L}{\partial \beta_{\Im,j}(t)} = -3\sum_{i=1}^{MN}\frac{\Im[a_{g(i)}^*(\psi_j)b_{f(i)}^*(\omega_j)n_i(t)]}{\gamma^2 + |n_i(t)|^2}$$

$$j = 1,\ldots,q, \quad t = 1,\ldots,S. \tag{69}$$

In the following derivations, we extensively use the assumption in Section IV, which states that the noise samples are spatially and temporally independent, and the Proposition 1 which states that the noise phase is uniformly distribuited in $[0,2\pi]$, in order to get simplifications in the expressions

$$\mathcal{E}\left\{\left(\frac{\partial L}{\partial \psi_j}\right)\left(\frac{\partial L}{\partial \psi_k}\right)\right\}$$

$$= 9\mathcal{E}\left\{\sum_{t=1}^{S}\sum_{i=1}^{MN}\sum_{t'=1}^{S}\sum_{i'=1}^{MN}\frac{\Re[\beta_j^*(t)b_{f(i)}^*(\omega_j)(d_{g(i)}^a(\psi_j))^* n_i(t)]}{\gamma^2 + |n_i(t)|^2} \times \frac{\Re[\beta_k^*(t')b_{f(i')}^*(\omega_k)(d_{g(i')}^a(\psi_k))^* n_{i'}(t')]}{\gamma^2 + |n_{i'}(t')|^2}\right\}$$

$$= 9\mathcal{E}\left\{\sum_{t=1}^{S}\sum_{i=1}^{MN}\frac{\Re[\beta_j^*(t)b_{f(i)}^*(\omega_j)(d_{g(i)}^a(\psi_j))^* n_i(t)]}{\gamma^2 + |n_i(t)|^2} \times \frac{\Re[\beta_k^*(t)b_{f(i)}^*(\omega_k)(d_{g(i)}^a(\psi_k))^* n_i(t)]}{\gamma^2 + |n_i(t)|^2}\right\}. \tag{70}$$

Setting

$$\phi_i^n(t) = \arctan\left(\frac{\Im[n_i(t)]}{\Re[n_i(t)]}\right),$$

$$\phi_\beta^j(t) = \arctan\left(\frac{\beta_{\Im,j}(t)}{\beta_{\Re,j}(t)}\right),$$

$$\phi_i^b(\omega_j) = \arctan\left(\frac{\Im[b_i(\omega_j)]}{\Re[b_i(\omega_j]}\right), \quad \text{and}$$

$$\phi_i^a(\psi_j) = \arctan\left(\frac{\Im[a_i(\psi_j)]}{\Re[a_i(\psi_j)]}\right)$$

for $i = 1,\ldots,MN$, $j = 1,\ldots,q$, $t = 1,\ldots,S$, and using the fact that $\{|a_i(\psi_j)| = 1,\ i = 1,2,\ldots,N\}$ and $\{|b_i(\omega_j)| = 1,\ i = 1,2,\ldots,M\}$, we obtain

$$\mathcal{E}\left\{\left(\frac{\partial L}{\partial \psi_j}\right)\left(\frac{\partial L}{\partial \psi_k}\right)\right\}$$

$$= 9\sum_{t=1}^{S}\sum_{i=1}^{MN}\mathcal{E}\left\{\frac{|n_i(t)|^2}{(\gamma^2 + |n_i(t)|^2)^2}\right\} \times |\beta_j(t)|\,|\beta_k(t)|\,|d_{g(i)}^a(\psi_j)|\,|d_{g(i)}^a(\psi_k)|$$
$$\times \mathcal{E}\left\{\cos(-\phi_\beta^j(t)) - \phi_{g(i)}^a(\psi_j) - \frac{\pi}{2} - \phi_{f(i)}^b(\omega_j) + \phi_i^n(t)) \times \cos(-\phi_\beta^k(t)) - \phi_{g(i)}^a(\psi_k) - \frac{\pi}{2} - \phi_{f(i)}^b(\omega_k) + \phi_i^n(t))\right\}$$

$$= 9\sum_{t=1}^{S}\sum_{i=1}^{MN}|\beta_j(t)|\,|\beta_k(t)|\,|d_{g(i)}^a(\psi_j)|\,|d_{g(i)}^a(\psi_k)| \times \mathcal{E}\left\{\frac{|n_i(t)|^2}{(\gamma^2 + |n_i(t)|^2)^2}\right\}$$
$$\times \tfrac{1}{2}\cos(-\phi_\beta^j + \phi_\beta^k - \phi_{g(i)}^a(\psi_j) + \phi_{g(i)}^a(\psi_k) - \phi_{f(i)}^b(\omega_j) + \phi_{f(i)}^b(\omega_k))$$

$$= \frac{3}{5\gamma^2}\sum_{t=1}^{S}\sum_{i=1}^{MN}\Re\{\beta_j^*(t)(d_{g(i)}^a(\psi_j))^* b_{f(i)}^* \times (\omega_j)\beta_k(t)d_{g(i)}^a(\psi_k)b_{f(i)}(\omega_k)\}$$

$$= \sum_{t=1}^{S}\Re\{\beta_j^*(t)\beta_k(t)[(\mathbf{b}(\omega_j)\otimes\mathbf{d}_a(\psi_j))^H \cdot (\mathbf{b}(\omega_k)\otimes\mathbf{d}_a(\psi_k))]\}$$

$$j,k = 1,\ldots,q. \tag{71}$$

Equation (71) can be written compactly as

$$\mathcal{E}\left\{\left(\frac{\partial L}{\partial \psi}\right)\left(\frac{\partial L}{\partial \psi}\right)^T\right\} = \frac{3}{5\gamma^2}\sum_{t=1}^{S}\Re\{\beta^H(t)\mathbf{D}_{b\otimes d_a}^H\mathbf{D}_{b\otimes d_a}\beta(t)\}. \tag{72}$$

Similarly,

$$\mathcal{E}\left\{\left(\frac{\partial L}{\partial \omega}\right)\left(\frac{\partial L}{\partial \omega}\right)^T\right\} = \frac{3}{5\gamma^2}\sum_{t=1}^{S}\Re\{\beta^H(t)\mathbf{D}_{d_b\otimes a}^H\mathbf{D}_{d_b\otimes a}\beta(t)\} \quad (73)$$

and

$$\mathcal{E}\left\{\left(\frac{\partial L}{\partial \omega}\right)\left(\frac{\partial L}{\partial \psi}\right)^T\right\} = \frac{3}{5\gamma^2}\sum_{t=1}^{S}\Re\{\beta^H(t)\mathbf{D}_{b\otimes d_a}^H\mathbf{D}_{d_b\otimes a}\beta(t)\}. \quad (74)$$

Now,

$$\begin{aligned}\mathcal{E}\left\{\left(\frac{\partial L}{\partial \gamma}\right)^2\right\} &= \left(\frac{MNS}{\gamma}\right)^2 - 6MNS\sum_{t=1}^{S}\sum_{i=1}^{MN} \times \mathcal{E}\left\{\frac{1}{\gamma^2+|n_i(t)|^2}\right\} + 9\gamma^2\sum_{t=1}^{S}\sum_{i=1}^{MN}\sum_{t'=1}^{S}\sum_{i'=1}^{MN} \\ &\quad \times \mathcal{E}\left\{\frac{1}{\gamma^2+|n_i(t)|^2}\frac{1}{\gamma^2+|n_i'(t')|^2}\right\} \\ &= \left(\frac{MNS}{\gamma}\right)^2 - \frac{6(MNS)^2}{3\gamma^2} \\ &\quad + 9\gamma^2\sum_{t=1}^{S}\sum_{i=1}^{MN}\mathcal{E}\left\{\frac{1}{(\gamma^2+|n_i(t)|^2)^2}\right\} \\ &\quad + 9\gamma^2\underbrace{\sum_{t=1}^{S}\sum_{i=1}^{MN}\sum_{t'=1}^{S}\sum_{i'=1}^{MN}}_{t\neq t' \text{ or } i\neq t'}\mathcal{E}\left\{\frac{1}{\gamma^2+|n_i(t)|^2}\right\} \\ &\quad \times \mathcal{E}\left\{\frac{1}{\gamma^2+|n_{i'}(t')|^2}\right\} \\ &= \frac{MNS}{\gamma^2} - \frac{2(MNS)^2}{\gamma^2} \\ &\quad + \frac{9\gamma^2 MNS(MNS-1)}{5\gamma^4} \\ &= \frac{4}{5}\frac{MNS}{\gamma^2}. \end{aligned} \quad (75)$$

In addition,

$$\begin{aligned}\mathcal{E}&\left\{\left(\frac{\partial L}{\partial \beta_{\Re,j}(t)}\right)\left(\frac{\partial L}{\partial \beta_{\Re,k}(t')}\right)\right\} \\ &= 9\mathcal{E}\left\{\sum_{i=1}^{MN}\sum_{i'=1}^{MN}\frac{\Re[b_{f(i)}^*(\omega_j)a_{g(i)}^*(\psi_j)n_i(t)]}{\gamma^2+|n_i(t)|^2} \times \frac{\Re[b_{f(i')}^*(\omega_k)a_{g(i')}^*(\psi_k)n_{i'}(t')]}{\gamma^2+|n_{i'}(t')|^2}\right\} \\ &= 9\mathcal{E}\left\{\sum_{i=1}^{MN}\frac{\Re[b_{f(i)}^*(\omega_j)(a_{g(i)}^*(\psi_j)n_i(t)]}{\gamma^2+|n_i(t)|^2} \times \frac{\Re[b_{f(i)}^*(\omega_k)a_{g(i)}^*(\psi_k)n_i(t)]}{\gamma^2+|n_i(t)|^2}\right\}\delta_{t,t'} \end{aligned} \quad (76)$$

where

$$\delta_{t,t'} = \begin{cases} 1 & \text{for } t = t' \\ 0 & \text{for } t \neq t' \end{cases}.$$

Continuing, we have

$$\begin{aligned}\mathcal{E}&\left\{\left(\frac{\partial L}{\partial \beta_{\Re,j}(t)}\right)\left(\frac{\partial L}{\partial \beta_{\Re,k}(t')}\right)\right\} \\ &= 9\sum_{i=1}^{MN}\mathcal{E}\left\{\frac{|n_i(t)|^2}{(\gamma^2+|n_i(t)|^2)^2}\right\} \\ &\quad \times \mathcal{E}\{\cos(-\phi_{g(i)}^a(\psi_j) - \phi_{f(i)}^b(\omega_j) + \phi_i^n(t)) \\ &\qquad \times \cos(-\phi_{g(i)}^a(\psi_k)\phi_{f(i)}^b(\omega_k) + \phi_i^n(t))\}\delta_{t,t'} \\ &= 9\sum_{i=1}^{MN}|\beta_j(t)\mathcal{E}\left\{\frac{|n_i(t)|^2}{(\gamma^2+|n_i(t)|^2)^2}\right\} \\ &\quad \times \tfrac{1}{2}\cos(-\phi_{g(i)}^a(\psi_j) + \phi_{g(i)}^a(\psi_k) \\ &\qquad - \phi_{f(i)}^b(\omega_j) + \phi_{f(i)}^b(\omega_k))\delta_{t,t'} \\ &= \frac{3}{5\gamma^2}\sum_{i=1}^{MN}\Re\{a_{g(i)}^*(\psi_j))b_{f(i)}^*(\omega_j)a_{g(i)}(\psi_k)b_{f(i)}(\omega_k)\}\delta_{t,t'} \\ &= \Re\{(\mathbf{b}(\omega_j)\otimes\mathbf{a}(\psi_j))^H\cdot(\mathbf{b}(\omega_k)\otimes\mathbf{a}(\psi_k))\}\delta_{t,t'} \\ &\qquad j,k = 1,\ldots,q, \quad t,t' = 1,\ldots,S. \end{aligned} \quad (77)$$

Equation (77) can be written compactly as

$$\mathcal{E}\left\{\left(\frac{\partial L}{\partial \beta_{\Re}(t)}\right)\left(\frac{\partial L}{\partial \beta_{\Re}(t')}\right)^T\right\} = \frac{3}{5\gamma^2}\Re\{\mathbf{D}_{b\otimes a}^H\mathbf{D}_{b\otimes a}\}\delta_{t,t'} \qquad t,t' = 1,\ldots,S. \quad (78)$$

Similarly, we have

$$\mathcal{E}\left\{\left(\frac{\partial L}{\partial \beta_{\Im}(t)}\right)\left(\frac{\partial L}{\partial \beta_{\Im}(t')}\right)^T\right\} = \frac{3}{5\gamma^2}\Re\{\mathbf{D}_{b\otimes a}^H\mathbf{D}_{b\otimes a}\}\delta_{t,t'} \qquad t,t' = 1,\ldots,S \quad (79)$$

$$\mathcal{E}\left\{\left(\frac{\partial L}{\partial \beta_{\Re}(t)}\right)\left(\frac{\partial L}{\partial \beta_{\Im}(t')}\right)^T\right\} = \frac{3}{5\gamma^2}\Im\{\mathbf{D}_{b\otimes a}^H\mathbf{D}_{b\otimes a}\}\delta_{t,t'} \qquad t,t' = 1,\ldots,S. \quad (80)$$

Also,

$$\mathcal{E}\left\{\left(\frac{\partial L}{\partial\psi_j}\right)\left(\frac{\partial L}{\partial\beta_{\Re,k}(t)}\right)\right\}$$

$$= 9\mathcal{E}\left\{\sum_{t'=1}^{S}\sum_{i'=1}^{MN}\sum_{i=1}^{MN}\frac{\Re[\beta_j^*(t')b_{f(i')}^*(\omega_j)(d_{g(i')}^a(\psi_j))^* n_{i'}(t')]}{\gamma^2+|n_{i'}(t')|^2}\times\frac{\Re[b_{f(i)}^*(\omega_k)a_{g(i)}^*(\psi_k)n_i(t)]}{\gamma^2+|n_i(t)|^2}\right\}$$

$$= 9\mathcal{E}\left\{\sum_{i=1}^{MN}\frac{\Re[\beta_j^*(t)b_{f(i)}^*(\omega_j)(d_{g(i)}^a(\psi_j))^* n_i(t)]}{\gamma^2+|n_i(t)|^2}\times\frac{\Re[b_{f(i)}^*(\omega_k)a_{g(i)}^*(\psi_k)n_i(t)]}{\gamma^2+|n_i(t)|^2}\right\}$$

$$= 9\sum_{i=1}^{MN}\mathcal{E}\left\{\frac{|n_i(t)|^2}{(\gamma^2+|n_i(t)|^2)^2}\right\}|\beta_j^*(t)|\,|d_{g(i)}^a(\psi_j)$$

$$\times\mathcal{E}\left\{\cos(-\phi_j^\beta(t)-\phi_{g(i)}^a(\psi_j)-\phi_{f(i)}^b(\omega_j)-\frac{\pi}{2}+\phi_i^n(t))\cos(-\phi_{g(i)}^a(\psi_k)-\phi_{f(i)}^b(\omega_k)+\phi_i^n(t))\right\}$$

$$= 9\sum_{i=1}^{MN}|\beta_j(t)|\mathcal{E}\left\{\frac{|n_i(t)|^2}{(\gamma^2+|n_i(t)|^2)^2}\right\}$$

$$\times\frac{1}{2}\cos\left(-\phi_j^\beta(t)-\phi_{g(i)}^a(\psi_j)+\phi_{g(i)}^a(\psi_k)-\phi_{f(i)}^b(\omega_j)+\phi_{f(i)}^b(\omega_k)-\frac{\pi}{2}\right)$$

$$= \frac{3}{5\gamma^2}\sum_{i=1}^{MN}\Re\{\beta_j^*(t)(d_{g(i)}^a(\psi_j))^* b_{f(i)}^*(\omega_j)a_{g(i)}(\psi_k)b_{f(i)}(\omega_k)\}\,\delta_{t,t'}$$

$$= \Re\{\beta_j^*(t)[(\mathbf{b}(\omega_j)\otimes\mathbf{d}_a(\psi_j))^H\cdot(\mathbf{b}(\omega_k)\otimes\mathbf{a}(\psi_k))]\}$$

$$j,k=1,\ldots,q,\quad t=1,\ldots,S. \tag{81}$$

Equation (81) can be expressed in compact form as

$$\mathcal{E}\left\{\left(\frac{\partial L}{\partial\psi}\right)\left(\frac{\partial L}{\partial\beta_\Re(t)}\right)^T\right\} = \frac{3}{5\gamma^2}\Re\{\beta^H(t)\mathbf{D}_{b\otimes d_a}^H\mathbf{D}_{b\otimes a}\}$$

$$t=1,\ldots,S. \tag{82}$$

Similarly,

$$\mathcal{E}\left\{\left(\frac{\partial L}{\partial\psi}\right)\left(\frac{\partial L}{\partial\beta_\Im(t)}\right)^T\right\} = \frac{3}{5\gamma^2}\Im\{\beta^H(t)\mathbf{D}_{b\otimes d_a}^H\mathbf{D}_{b\otimes a}\}$$

$$t=1,\ldots,S \tag{83}$$

and

$$\mathcal{E}\left\{\left(\frac{\partial L}{\partial\omega}\right)\left(\frac{\partial L}{\partial\beta_\Re(t)}\right)^T\right\} = \frac{3}{5\gamma^2}\Re\{\beta^H(t)\mathbf{D}_{d_b\otimes a}^H\mathbf{D}_{b\otimes a}\}$$

$$t=1,\ldots,S \tag{84}$$

$$\mathcal{E}\left\{\left(\frac{\partial L}{\partial\omega}\right)\left(\frac{\partial L}{\partial\beta_\Im(t)}\right)^T\right\} = \frac{3}{5\gamma^2}\Im\{\beta^H(t)\mathbf{D}_{d_b\otimes a}^H\mathbf{D}_{b\otimes a}\}$$

$$t=1,\ldots,S. \tag{85}$$

Finally, it can be easily shown that

$$\mathcal{E}\left\{\left(\frac{\partial L}{\partial\gamma}\right)\left(\frac{\partial L}{\partial\psi}\right)^T\right\} = 0 \tag{86}$$

$$\mathcal{E}\left\{\left(\frac{\partial L}{\partial\gamma}\right)\left(\frac{\partial L}{\partial\omega}\right)^T\right\} = 0 \tag{87}$$

$$\mathcal{E}\left\{\left(\frac{\partial L}{\partial\gamma}\right)\left(\frac{\partial L}{\partial\beta_\Re(t)}\right)^T\right\} = 0 \quad t=1,\ldots,S \tag{88}$$

$$\mathcal{E}\left\{\left(\frac{\partial L}{\partial\gamma}\right)\left(\frac{\partial L}{\partial\beta_\Im(t)}\right)^T\right\} = 0 \quad t=1,\ldots,S. \tag{89}$$

The Fisher Information Matrix can now be written as

$$\mathbf{J}(\eta) = \begin{bmatrix} \Gamma & 0 & 0 & \cdots & 0 & 0 & 0 & 0 \\ 0 & \Delta_\Re & \Delta_\Im & \cdots & \mathbf{0} & \mathbf{0} & \Omega_\Re(1) & \Omega_\Im(1) \\ 0 & -\Delta_\Im & \Delta_\Re & \cdots & \mathbf{0} & \mathbf{0} & \Gamma_\Re(1) & \Gamma_\Im(1) \\ \vdots & \vdots & \vdots & & \vdots & \vdots & \vdots & \vdots \\ 0 & \mathbf{0} & \mathbf{0} & \cdots & \Delta_\Re & \Delta_\Im & \Omega_\Re(S) & \Omega_\Im(S) \\ 0 & \mathbf{0} & \mathbf{0} & \cdots & -\Delta_\Im & \Delta_\Re & \Gamma_\Re(S) & \Gamma_\Im(S) \\ 0 & \Omega_\Re(1) & \Gamma_\Re(1) & \cdots & \Omega_\Re(S) & \Gamma_\Re(S) & \Sigma_{\psi^2} & \Sigma_{\psi\omega} \\ 0 & \Omega_\Im(1) & \Gamma_\Im(1) & \cdots & \Omega_\Im(S) & \Gamma_\Im(S) & \Sigma_{\psi\omega}^T & \Sigma_{\omega^2} \end{bmatrix} \tag{90}$$

where

$$\Gamma = \frac{4}{5}\frac{MNS}{\gamma^2} \tag{91}$$

and the following $q\times q$ matrices are used

$$\Delta_\Re = \Re\{\Delta\} = \frac{3}{5\gamma^2}\Re\{\mathbf{D}_{b\otimes a}^H\mathbf{D}_{b\otimes a}\} \tag{92}$$

$$\Delta_\Im = \Im\{\Delta\} = \frac{3}{5\gamma^2}\Im\{\mathbf{D}_{b\otimes a}^H\mathbf{D}_{b\otimes a}\} \tag{93}$$

$$\Omega_\Re(t) = \Re\{\omega(t)\} = \frac{3}{5\gamma^2}\Re\{\beta^H(t)\mathbf{D}_{b\otimes d_a}^H\mathbf{D}_{b\otimes a}\}$$

$$t=1,\ldots,S \tag{94}$$

$$\Omega_{\Im}(t) = \Im\{\omega(t)\} = \frac{3}{5\gamma^2}\Im\{\beta^H(t)\mathbf{D}^H_{b\otimes d_a}\mathbf{D}_{b\otimes a}\} \quad t = 1,\ldots,S \qquad (95)$$

$$\Gamma_{\Re}(t) = \Re\Gamma(t) = \frac{3}{5\gamma^2}\Re\{\beta^H(t)\mathbf{D}^H_{d_b\otimes a}\mathbf{D}_{b\otimes a}\} \quad t = 1,\ldots,S \qquad (96)$$

$$\Gamma_{\Im}(t) = \Im\Gamma(t) = \frac{3}{5\gamma^2}\Im\{\beta^H(t)\mathbf{D}^H_{d_b\otimes a}\mathbf{D}_{b\otimes a}\} \quad t = 1,\ldots,S \qquad (97)$$

$$\Sigma_{\psi^2} = \frac{3}{5\gamma^2}\sum_{t=1}^{S}\Re\{\beta^H(t)\mathbf{D}^H_{b\otimes d_a}\mathbf{D}_{b\otimes d_a}\beta(t)\} \qquad (98)$$

$$\Sigma_{\psi\omega} = \frac{3}{5\gamma^2}\sum_{t=1}^{S}\Re\{\beta^H(t)\mathbf{D}^H_{b\otimes d_a}\mathbf{D}_{d_b\otimes a}\beta(t)\} \qquad (99)$$

$$\Sigma_{\omega^2} = \frac{3}{5\gamma^2}\sum_{t=1}^{S}\Re\{\beta^H(t)\mathbf{D}^H_{d_b\otimes a}\mathbf{D}_{d_b\otimes a}\beta(t)\} \qquad (100)$$

Clearly,

$$\mathrm{CRB}(\gamma) = \frac{1}{\Gamma} = \frac{5}{4}\frac{\gamma^2}{MNS}. \qquad (101)$$

Now, let

$$\Xi = \begin{bmatrix} \Delta_{\Re}^{-1} & \Delta_{\Im}^{-1} \\ -\Delta_{\Im}^{-1} & \Delta_{\Re}^{-1} \end{bmatrix} \qquad (102)$$

$$\Upsilon(t) = \begin{bmatrix} \Omega_{\Re}(t) & \Omega_{\Im}(t) \\ \Gamma_{\Re}(t) & \Gamma_{\Im}(t) \end{bmatrix} \quad t = 1,\ldots,S \qquad (103)$$

and

$$\Sigma = \begin{bmatrix} \Sigma_{\psi^2} & \Sigma_{\psi\omega} \\ \Sigma_{\psi\omega}^T & \Sigma_{\omega^2} \end{bmatrix}. \qquad (104)$$

Using a standard result of the inverse of a partitioned matrix [33], the CRB for the parameters ψ and ω results

$$\mathrm{CRB}^{-1}(\psi,\omega) = \Sigma - [\Upsilon^T(1)\cdots\Upsilon(S)] \times \begin{bmatrix} \Xi & & \\ & \ddots & \\ & & \Xi \end{bmatrix} \begin{bmatrix} \Upsilon(1) \\ \vdots \\ \Upsilon(S) \end{bmatrix}. \qquad (105)$$

Equation (105) can be expressed as

$$\mathrm{CRB}(\psi,\omega) = \left[\Sigma - \sum_{t=1}^{S}\Upsilon^T(t)\Xi\Upsilon(t)\right]^{-1} \qquad (106)$$

and the proof is completed.

REFERENCES

[1] Brennan, L. E., and Reed, I. S. (1973)
Theory of adaptive radar.
IEEE Transactions on Aerospace and Electronic Systems, **AES-9** (1973), 237–252.

[2] Reed, I. S., Mallett, J. D., and Brennan, L. E. (1974)
Rapid convergence rate in adaptive arrays.
IEEE Transactions on Aerospace and Electronic Systems, **AES-10** (1974), 853–863.

[3] Kelly, E. J. (1986)
An adaptive detection algorithm.
IEEE Transactions on Aerospace and Electronic Systems, **AES-22** (Mar. 1986), 115–127.

[4] Raghavan, R. S. (1991)
A method for estimating parameters of K-distributed clutter.
IEEE Transactions on Aerospace Electronic Systems, **27** (Mar. 1991), 238–246.

[5] Sekine, M., and Mao, Y. (1990)
Weibull Radar Clutter.
London: Peter Peregrinus Ltd., 1990.

[6] Menon, M. V. (1963)
Estimation of the shape and scale parameters of the Weibull distribution.
Technometrics, **5** (1963), 175–182.

[7] Ballard, A. H. (1966)
Detection of radar signals in log-normal sea-clutter.
Technical report 7425-8509-T0-000, TRW Systems Doc., 1966.

[8] Kassam, S. A. (1976)
Asymptotically robust detection of a known signal in contaminated non-Gaussian noise.
IEEE Transactions on Information Theory, **IT-22** (1976), 22–26.

[9] Goldman, J. (1976)
Detection in the presence of spherically symmetric random vectors.
IEEE Transactions on Information Theory, **22** (1976), 52–59.

[10] Sangrton, K. J., and Gerlach, K. R. (1994)
Coherent detection of radar targets in a non-Gaussian background.
IEEE Transactions on Aerospace Electronic Systems, **30** (Apr. 1994), 330–340.

[11] Rangaswamy, M., Weiner, D., and Ozturk, A. (1993)
Non-Gaussian random vector identification using spherically invariant random processes.
IEEE Transactions on Aerospace Electronic Systems, **29** (Jan. 1993), 111–123.

[12] Izzo, L., and Tanda, M. (1993)
Array detection of random signals in spherically invariant noise.
Journal of the Acoustical Society of America, **94** (1993), 2682–2690.

[13] Izzo, L., and Tanda, M. (1995)
Constant false-alarm rate array detection of random signals in spherically invariant noise.
Journal of the Acoustical Society of America, **98** (1995), 931–937.

[14] Reed, I. S., Nikias, C. L., and Prasanna, V. (1996)
Multidisciplinary research on advanced high-speed, adaptive signal processing for radar sensors.
Technical report, University of Southern California, Jan. 1996.

[15] Nikias, C. L., and Shao, M. (1995)
Signal Processing with Alpha-Stable Distributions and Applications.
New York: Wiley, 1995.

[16] Titi, G., and Marshall, D. (1996)
The ARPA/NAVY Mountaintop program—Adaptive signal processing for airborne early warning radar.
In *Proceedings of ICASSP 1996*, Atlanta, GA, 1996, 1165–1169.

[17] Ward, J. (1994)
Space-time adaptive processing for airborne radar.
Technical report 1015, Lincoln Laboratory, Dec. 1994.

[18] Baranoski, E. J. (1995)
Improved pre-Doppler STAP algorithm for adaptive clutter nulling in airborne radars.
Presented at the *Twenty-Ninth Asilomar Conference on Signals, Systems and Computers*, Pacific Grove, CA, Oct. 30–Nov. 1, 1995.

[19] Kreithen, D. E., and Steinhardt, A. O. (1995)
Target detection in post-STAP undernulled clutter.
Presented at the *Twenty-Ninth Asilomar Conference on Signals, Systems and Computers*, Pacific Grove, CA, Oct. 30–Nov. 1, 1995.

[20] Tsakalides, P., Raspanti, R., and Nikias, C. L. (1996)
Joint target angle and Doppler estimation in interference modeled as a stable process.
In *Proceedings of the 30th Conference on Information Sciences and Systems*, Princeton, NJ, Mar. 20–22, 1996.

[21] Ward, J. (1995)
Cramér–Rao bounds for target angle and Doppler estimation with space-time adaptive processing radar.
Presented at the Twenty-Ninth Asilomar Conference on Signals, Systems and Computers, Pacific Grove, CA, Oct. 30–Nov. 1, 1995.

[22] Tsakalides, P., and Nikias, C. L. (1995)
Maximum likelihood localization of sources in noise modeled as a stable process.
IEEE Transactions on Signal Processing, **43** (Nov. 1995), 2700–2713.

[23] Tsakalides, P., and Nikias, C. L. (1996)
The robust covariation-based MUSIC (ROC-MUSIC) algorithm for bearing estimation in impulsive noise environments.
IEEE Transactions on Signal Processing, **44** (July 1996), 1623–1633.

[24] Cambanis, S., and Miamee, A. G. (1989)
On prediction of harmonizable stable processes.
Sankhyā: The Indian Journal of Statistics, **51** (1989), 269–294.

[25] Cambanis, S. (1983)
Complex symmetric stable variables and processes.
In *Contributions to Statistics: Essays in Honor of Norman L. Johnson* (P. Sen (Ed.)), New York: North-Holland, 1983, 63–79.

[26] DuMouchel, W. H. (1971)
Stable Distributions in Statistical Inference.
Ph.D. thesis, Dept. of Statistics, Yale University, New Haven, CT, 1971.

[27] Brorsen, B. W., and Yang, S. R. (1990)
Maximum likelihood estimates of symmetric stable distribution parameters.
Commun. Statist.-Simul., **19** (1990), 1459–1464.

[28] Paulson, A. S., Holcomb, E. W., and Leitch, R. A. (1975)
The estimation of the parameters of the stable laws.
Biometrika, **62** (1975), 163–170.

[29] Zolotarev, V. M. (1980)
Statistical estimates of the parameters of stable laws.
Mathematical Statistics: Banach Center Pub., **6** (1980), 359–376.

[30] McCulloch, J. H. (1986)
Simple consistent estimators of stable distribution parameters.
Commun. Statist.-Simul., **15** (1986), 1109–1136.

[31] Fama, E. F., and Roll, R. (1968)
Some properties of symmetric stable distributions.
Journal of the American Statistical Association, **63** (1968), 817–836.

[32] Ma, X., and Nikias, C. L. (1995)
Parameter estimation and blind channel identification for impulsive signal environments.
IEEE Transactions on Signal Processing, **43** (Dec. 1995), 2884–2897.

[33] Scharf, L. L. (1991)
Statistical Signal Processing: Detection, Estimation and Time Series Analysis.
Menlo Park: Addison-Wesley, 1991.

[34] Ottersten, B., Viberg, M., Stoica, P., and Nehorai, A. (1993)
Exact and large sample maximum likelihood techniques for parameter estimation and detection in array processing.
In S. Haykin, J. Litva, and T. J. Shepherd (Eds.), *Radar Array Processing.*
New York: Springer-Verlag, 1993.

[35] Tsakalides, P., and Nikias, C. L. (1995)
Direction finding with fractional lower-order statistics.
Presented at the 1995 Adaptive Sensor Array Processing (ASAP) Workshop, MIT Lincoln Laboratory, Lexington, MA, Mar. 15–17 1995.

[36] Luenberger, D. G. (1984)
Linear and Nonlinear Programming (2nd ed.).
Menlo Park: Addison-Wesley, 1984.

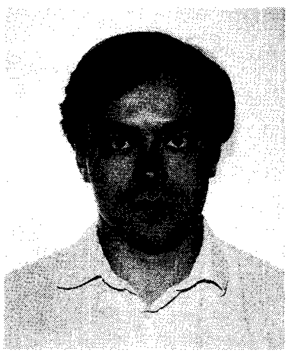

Panagiotis Tsakalides (S'93—M'95) received the Diploma in electrical engineering from the Aristotle University of Thessaloniki, Greece, in 1990. He obtained the M.S. degree in computer engineering in 1991 and the Ph.D. degree in electrical engineering in 1995, both from the University of Southern California (USC), Los Angeles.

In 1996, he became a Research Assistant Professor with the Signal and Image Processing Institute, Department of Electrical Engineering–Systems, at USC. In Dec. 1998 he joined the VLSI Design Laboratory, University of Patras, Greece. His general research interests lie in the area of statistical signal processing with emphasis in estimation and detection theory, and applications in array processing for communications, sonar, and radar problems.

Over the last five years Dr. Tsakalides has published more that 30 technical journal and conference papers.

Raffaele Raspanti was born in Florence, Italy on March 13, 1970. He received the Diploma in electrical engineering from the University of Florence, Florence, Italy in 1996.

From September 1995 until March 1996 he was a research associate with the Signal and Image Processing Institute at the University of Southern California in Los Angeles, working on his Diploma thesis. Since then he has been living in Rome working for Andersen Consulting on data modeling, business integration, and system building.

Chrysostomos L. Nikias (S'79—M'81—SM'87—F'97) received a Diploma in mechanical and electrical engineering from the National Technical University of Athens, Greece in 1977 and both the M.S. and Ph.D. degrees in electrical engineering from the State University of New York at Buffalo, NY in 1980 and 1982, respectively.

He is currently Professor of Electrical Engineering–Systems at the University of Southern California, Associate Dean of Engineering and Director of USCs Integrated Media Systems Center (IMSC). Prior to that he held academic appointments at Northeastern University in Boston and the University of Connecticut in Storrs.

Dr. Nikias is the recipient of both the 1993 Outstanding Teacher Award from the National Technological University (TV University in USA) and the "Fred W. Ellersick Award of Outstanding Unclassified Paper at Military Communications (MILCOM)'92." He is also the recipient of the 1987 IEEE Signal Processing best paper award. He is a member of the California Council on Science and Technology. He is the author of over 100 published journal papers, 4 textbooks and 7 patents.